*URSI-RCRS 2024, ARIES/GEHU, Bhimtal, India, 22 - 25 October, 2024*

# Retrieval of Venus' Ionospheric Profile from Radio Science Experiment Onboard Akatsuki

Tirtha J. Kalita*(1), Varun Sheel(1) and S.M. Sharma (1),(2)
(1) Physical Research Laboratory, Ahmedabad, India, 380059, https://www.prl.res.in
(2) Indian Institute of Technology, Gandhinagar

## Abstract

We retrieved the Venusian Ionospheric profiles from the Radio Science Experiment onboard Akatsuki spacecraft of JAXA, also known as Venus Climate Orbiter (VCO). A 8.4 GHz downlink radio signal transmitted from the Ultra Stable Oscillator (USO) onboard the spacecraft is received at the 32 m antenna at Indian Deep Space Network (IDSN), Byalalu. The received signal is heterodyned and sampled at the ground station and further digitized as data packets is used to apply a retrieval algorithm to estimate the frequency shift due to path delay experienced by the traveling radio ray while passing through the ionospheric and atmospheric medium of Venus. A peak electron number density of 2 - 4.5 $m^{-3}$ is observed at $V_2$ layer (~140 km). $V_1$ peak density is observed at ~120-130 km. The sporadic $V_0$ layer observation is also a major highlight of this work. We also made comparisons of our results obtained with retrievals from data received at the two ground stations ( IDSN, Byalalu and UDSC, Japan) with results from Venus Express for similar SZA conditions for validation.

## 1. Introduction

### 1.1 The Ionosphere of Venus

The ionosphere of Venus is characterized in four different layers: $V_3$, $V_2$, $V_1$ and $V_0$. The dayside ionosphere has a dominant ion layer between 135-145 km peaking around 140 km. This layer, called $V_2$ , primarily constitutes $O_2^+$ ions produced by the charge exchange reactions of $CO_2^+$ ions, with $CO_2^+$ ions being produced by solar EUV radiation and secondary ionization by energetic electrons [3,4,5]. A secondary layer produced by the soft X-rays and secondary electron impact ionization [6,7] peaks at about 125 km, known as the $V_1$ layer [4]. A sporadic $V_0$ layer has been detected below 120 km, which appears to be independent of solar activity and SZA [8,9]. The mechanisms underlying the occurrence of this layer remain unresolved and are an ongoing subject of investigation. A ledge-like layer formed due to diffusion above 180 km, with no dominant peak was reported from VeRa measurements [2], termed as $V_3$ layer, dominated by $O^+$ ions. However, the existence and source of the nighttime ionosphere is still not well understood. Transportation of superthermal electrons/$O^+$ ions from higher altitudes from the dayside is speculated to produce ions in the nightside by secondary impact ionization [13].

### 1.2 Radio Occultation Technique

The full structure of the ionosphere can only be assessed by remote sensing radio occultation methods. It is a powerful technique that utilizes the concept of path delay experienced by a radio ray due to refraction while propagating through different media to retrieve atmospheric pressure, temperature, sulfuric acid vapor mixing ratio, electron and neutral number densities. The Venus ionosphere was first detected by the radio occultation (RO) experiment on Mariner -5 in 1967 [1]. The dayside profiles showed a peak of electron density between $5 \times 10^5$ $cm^{-3}$ to $6\times 10^5$ $cm^{-3}$ near 142 km. Also, a minor layer approximately 15 km below the maximum ionization was found [1]. Electron density profiles were subsequently derived from similar measurements by spacecraft like Mariner 10, Venera 9, 10, 15, 16, Pioneer Venus Orbiter (PVO), and Venus Express (VEX) etc. These missions contributed significantly in enhancing the understanding of the Venus ionosphere [2,6,10]. Venus Express Radio Science (VeRa) experiment provided more than 200 RO profiles during 2005-2013 [6] and contributed significantly toward the current understanding of Venus ionosphere. At present, the Akatsuki spacecraft is orbiting Venus, providing additional electron density profiles and further enriching our insights into the Venusian ionosphere.

## 2. Data acquisition and Methodology

### 2.1 Data Source

The 8.4 GHz radio signal transmitted from the Ultra Stable Oscillator (USO), sitting on the spacecraft is received at the ground station at Indian Deep Space Network (IDSN), Byalalu in the open loop mode. The signal is then heterodyned using a local oscillator and sampled at 200 KHz rate. Data is recorded in an internationally accepted raw data exchange format (RDEF). RDEF data comprises two sections: Section 1 is the header and contains information about Section 2 (including data size) which contains the data. Data size depends upon the sampling rate and is stored in baseband complex form of in-phase and in-quadrature components in the time domain.

### 2.2 Data Processing

Analysis of data consists of two major components:

1. Estimation of frequency residuals
2. Obtaining and profiling atmospheric parameters from frequency residuals

#### 2.2.1 Frequency Residual Estimation

The phase of the residual signal is computed using:

$$\Psi_{res} = (\Psi_S + \Psi_{LO}) - \Psi_{DL} - \Psi_{str} \quad (1)$$

Where, $\Psi_{res}$ is the residual signal phase, $\Psi_S$ is the sampled signal phase, $\Psi_{LO}$ is the phase of the Local Oscillator, $\Psi_{DL}$ is the phase of the downlink signal at the USO and $\Psi_{str}$ is the phase of the straight line doppler.

The sampled I and Q data is used to calculate the phase and amplitude of the signal. The Local Oscillator (LO) phase is calculated to reconstruct the sky frequency using product information available for each data record. The sky frequency is the received frequency at the ground station antenna. Phase of the downlink signal is also computed using the header description.

The straight line doppler is induced because of the relative motion between the spacecraft and the receiver ground station. We used the SPICE toolkit by NAIF (Navigation Ancillary Information Facility, NASA) to calculate the positions and velocities of both the VCO and IDSN32 with respect to the solar system barycenter (SSB) in the J2000 frame of reference. The relationship between a transmitted frequency $f_A$ and a received frequency $f_B$ is [11]

$$\frac{f_B(t_B)}{f_A(t_A)} = \frac{1 - \frac{v_B(t_B).\hat{n}_B(t_B)}{c} - \frac{U_B(t_B)}{c^2} + \frac{v_B(t_B)^2}{2c^2}}{1 - \frac{v_A(t_A).\hat{n}_A(t_A)}{c} - \frac{U_A(t_A)}{c^2} + \frac{v_A(t_A)^2}{2c^2}} \quad (2)$$

Here $v_B(t_B)$ is the velocity of the receiver at reception time $t_B$, $\hat{n}_B(t_B)$is the unit vector along which the radio wave propagates into the receiver, $U_B(t_B)$ is the gravitational potential at the receiver, $v_A(t_A)$ is the velocity of the transmitter, $\hat{n}_A(t_A)$ is the unit vector along which the radio wave propagates away from the transmitter, and $U_B(t_B)$ is the gravitational potential at the transmitter. This expression is accurate to order $(v/c)^2$.

Using Eq.(2), we calculated the phase of the straight line doppler and applied Eq.(1) to compute the residual signal phase. The signal is reconstructed using the amplitude and phase information and removal of any DC bias present is applied.

The residual signal is resampled with a sample size of $2^{12}$, to increase the time resolution from 1 sec to ~0.082 sec. This takes care of the doppler spectrum broadening due to change in Line of Sight (LOS) velocity as well as the FFZ correction [12]. We applied a hamming window to each sample packet to avoid spectral leakage. Then FFT was applied to the signal with interpolation of $2^{10}$ points in each frequency bin. Finally a gaussian fit is applied to the power spectrum to estimate frequency residuals. Lastly a polynomial fit was applied by taking initial 10-15 min data as baseline and removing it from the entire time series. A running average of 12 points (each 1 sec data was divided into 12 parts) was also taken to remove short scale fluctuations. Fig.1(a) showing the final residual obtained for the ingress occultation period while Fig.1(b) is a zoomed portion for the ionospheric shift.

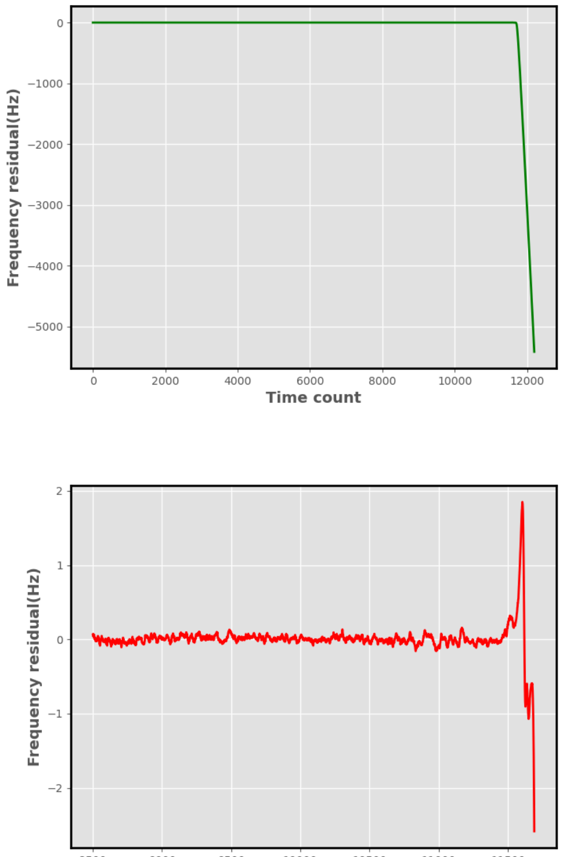


**Figure 1.** (a) Frequency residual w.r.t earth reception time for complete ingress period; (b) Frequency shift due to the ionosphere of Venus, for DOY 190, 2017. Here each time count corresponds to 0.082 sec.

### 2.2.2 Electron Density from Frequency Residuals

Fig.2 illustrates the geometry of the radio occultation observation.

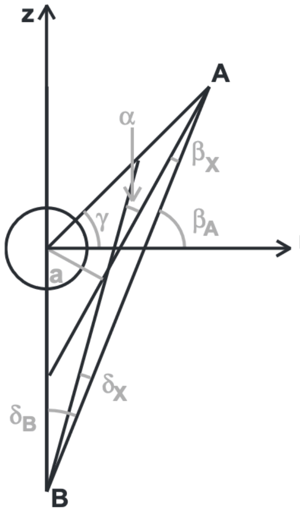


**Figure 2.** Geometry for an occultation involving transmitter A, receiver B, and target object P at the origin. credit: Withers et al. (2014)

The point A and B demonstrate the position of the center of mass of the transmitter ($x_A$) and the tracking station ($x_B$) at time $t_A$, $t_B$ respectively. The point of closest approach of the radio ray to the center of the target object P is $x_0$ and the time at which this radio signal is at this position is $t_0$. The time of closest approach to the planet $t_0$ and state vectors of the target object at that time is calculated using ephemeris data from SPICE. Similarly, positions and velocities of VCO, IDSN at their respective transmission and reception time are estimated.

If there is no refraction at the target object P. In this case, the radio signal travels directly from the transmitter to the receiver and the unit vectors $\hat{n}_A(t_A)$ and $\hat{n}_B(t_B)$ are equal. These two are labeled as $\hat{n}_{A,Direct}(t_A)$ and $\hat{n}_{B,Direct}(t_B)$. The received radio frequency is $f_{B,Direct}(t_B)$. In case of refraction at the target object these two unit vectors are different and labeled as the "occultation" unit vectors $\hat{n}_{A,Occ}(t_A)$ and $\hat{n}_{B,Occ}(t_B)$. Now the received radio frequency is $f_{B,Occ}(t_B)$. The difference between $f_{B,Occ}(t_B)$ and $f_{B,Direct}(t_B)$ is known as the frequency residual, $\Delta f\ (t_B)$. It can be related as[11]

$$\frac{\Delta f\ (t_B)}{f_A(t_A)} = \frac{1-\frac{v_B(t_B).\hat{n}_{B,Occ}(t_B)}{c}-\frac{U_B(t_B)}{c^2}+\frac{v_B(t_B)^2}{2c^2}}{1-\frac{v_A(t_A).\hat{n}_{A,Occ}(t_A)}{c}-\frac{U_A(t_A)}{c^2}+\frac{v_A(t_A)^2}{2c^2}} - \frac{1-\frac{v_B(t_B).\hat{n}_{B,Direct}(t_B)}{c}-\frac{U_B(t_B)}{c^2}+\frac{v_B(t_B)^2}{2c^2}}{1-\frac{v_A(t_A).\hat{n}_{A,Direct}(t_A)}{c}-\frac{U_A(t_A)}{c^2}+\frac{v_A(t_A)^2}{2c^2}} \quad (3)$$

But in order for a particular radio ray to remain confined to the plane outlined in Fig. 2, the frame of reference needed to be converted to a relevant r-z plane which is done according to the method described in Withers et al.(2014)[11]. This method enables us to calculate the bending angle and impact parameter as a function of time using Eq.(3) and the geometry of the occultation. An Abel Transform is then applied to determine the refractive index of the medium.

$$\pi ln\, \mu(R_0) = \int_{a=a_0}^{a=\infty} ln\left\{\frac{a}{a_0} + \sqrt{\left(\frac{a}{a_0}\right)^2 - 1}\right\}\frac{d\alpha}{da}da \quad (4)$$

Where, $R_0$ is the distance of closest approach, $\alpha$ is the bending angle and $a$ is the impact parameter.

The refractivity and radial distance is calculated from the refractive index. For typical radio occultation experiments in planetary ionospheres, refractivity $\nu_e$ satisfies

$$\nu_e = -\frac{N_e e^2}{8\pi^2 m_e \epsilon_0 f^2} \quad (5)$$

Thus, electron number density is calculated as a function of radial distance from the center of the planet.

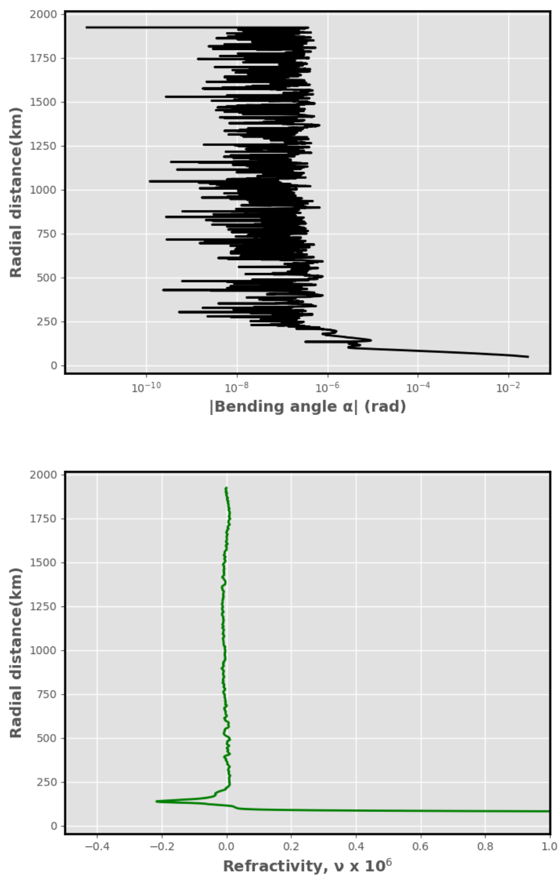


**Figure 3.**(a)Bending angle profile; (b) Refractivity profile for Venusian ionosphere/atmosphere for DOY 190, 2017. Here, the radius of Venus is taken as 6051.8 km.

## 3. Results and summary

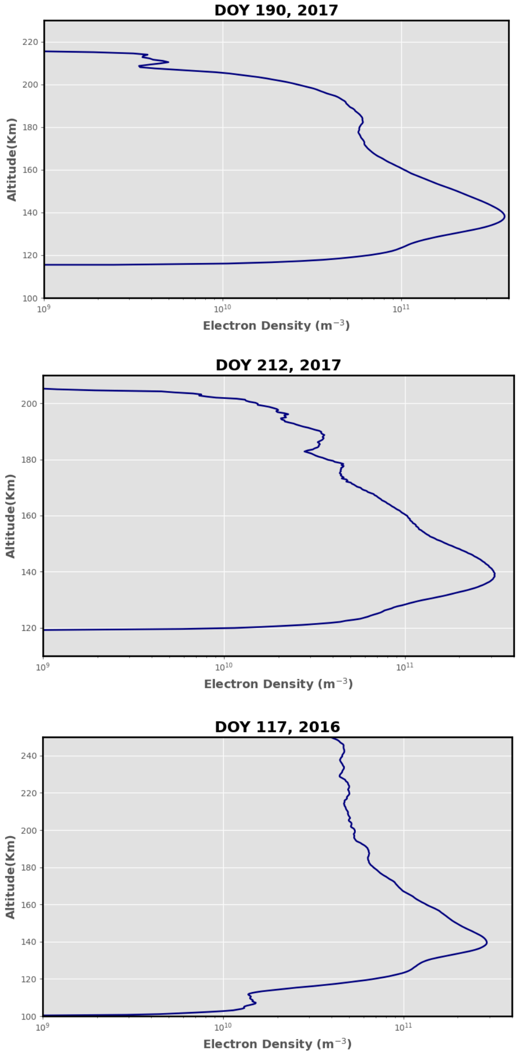


**Figure 4.** Electron density profiles from Akatsuki for (a) DOY 190, 2017 ; (b) DOY 212, 2017 and (c) DOY 117, 2016.

Both $V_1$ and $V_2$ are observed to be peaking at the same height ($V_1$~ 140 km and $V_2$ ~ 125 km) in all three cases suggesting minimal influence of solar activity and SZA on peak altitudes. While Fig. 4(c) differs from 4(a) and 4(b), above the $V_2$ layer where it is showing a ledge-like structure suggesting further analysis.

Additionally, the third profile reveals the presence of the $V_0$ layer at ~109 km. This layer appears to be completely independent of solar ionization, suggesting it is a sporadic layer. The identification of the $V_0$ layer in Akatsuki data highlights its unique nature and provides valuable insights into the complex electron density structure in Venus' ionosphere.

## 4. Acknowledgements


We would like to express our sincere gratitude to Prof. Martin Pätzold and Dr. Janusz Oschlisniok for their great support in this work. We would also like to thank Indian Deep Space Network, Byalalu ground station for necessary data support.


## 5. References


1. Kliore, A., Levy, G. S.et al. (1967). Atmosphere and Ionosphere of Venus from Mariner V S-bandRadio OccultationMeasurements.*Science*,158(3809),1683-1688. https://doi.org/10.1126/science.158.3809.1683

2. Pätzold, M., Häusler et al.(2007). The structure of Venus' middle atmosphere and ionosphere. 450, 657-660. https://doi.org/10.1038/nature06239

3.Ambili, K. M., Babu, S. S., & Choudhary, R. K. (2019). On the relative roles of the neutral density and photochemistry on the solar zenith angle variations in the V2 layer characteristics of the Venus ionosphere under different solar activity conditions. *Icarus*, *321*, 661–670. https://doi.org/10.1016/j.icarus.2018.12.001

4.Fox, J. L., & Kasprzak, W. T. (2007). Near-terminator Venus ionosphere: Evidence for a dawn/dusk asymmetry in the thermosphere. *Journal of Geophysical Research*, *112*(E9), E09008. https://doi.org/10.1029/2007je002899

5.Peter, K., Pätzold, M., Molina-Cuberos, G., Witasse, O., González-Galindo, F., Withers, P., et al. (2014). The dayside ionosphere of Mars andVenus: Comparing a one-dimensional photochemical model with Mars (Mars Express) and VeRa (Venus Express) observations. *Icarus*, *233*,66–82. https://doi.org/10.1016/j.icarus.2014.01.028

6.Gérard, J.-C., Bougher, S. W., López-Valverde, M. A., Pätzold et al. (2017). Aeronomy of the Venus upper atmosphere.*Space Science Reviews*,*212*(3),1617–1683. https://doi.org/10.1007/s11214-017-0422-0

7. Peter, K., Pätzold, M. et al. (2014). The dayside ionosphere of Mars and Venus: Comparing a one-dimensional photochemical model with Mars (Mars Express) and VeRa (Venus Express) observations. *Icarus*, *233*,66–82. https://doi.org/10.1016/j.icarus.2014.01.028

8. Pätzold, M., Tellmann, S., Häusler, B., Bird, M. K., Tyler, G. L., Christou, A. A., & Withers, P. (2009). A sporadic layer in the Venus lower ionosphere of meteoric origin. *Geophysical Research Letters*, *36*(5), L05203. https://doi.org/10.1029/2008gl035875

9.Tripathi, K., Choudhary, R.K., Ambili, K.M., Imamura, T., Ando, H. (2022). Characteristic Features of $V_0$ Layer in the Venus Ionosphere as Observed by the Akatsuki Orbiter: Evidence for Its Presence During the Local Noon and Post-Sunset Conditions. *Geophysical Research Letters*, 49(7), 8. https://doi.org/10.1029/2022GL097824

10. Brace, L. H., & Kliore, A. J. (1991). The structure of the Venus ionosphere. *Space Science Reviews*, *55*(1 - 4), 81–163. https://doi.org/10.1007/bf00177136

11.Withers, P., Moore, L., Cahoy, K., Beerer, I. (2014). How to process radio occultation data: 1. From time series of frequency residuals to vertical profiles of atmospheric and ionospheric properties.*Planetary and Space Science*, 101, 77-88. http://dx.doi.org/10.1016/j.pss.2014.06.011

12. Tripathi, K., Choudhary, R.K., Jayalal, L. (2022). On the estimation of frequency residuals in the radio occultation experiment. *MNRAS*, 517,776-786. https://doi.org/10.1093/mnras/stac2653

13.Fox, J. L. (2011). The post-terminator ionosphere of Venus.*Icarus*,*216*(2),625–639. https://doi.org/10.1016/j.icarus.2011.09.020